

HU-EP-14/03

Two-colour QCD at non-zero temperature in the presence of a strong magnetic field

M. Müller-Preussker^{*†}, B. Petersson, A. Schreiber

Humboldt-Universität zu Berlin, Institut für Physik, 12489 Berlin, Germany

*E-mail: mmp@physik.hu-berlin.de,
bengt.petersson@physik.hu-berlin.de,
alexander.schreiber@physik.hu-berlin.de*

E.-M. Ilgenfritz

Joint Institute for Nuclear Research, VBLHEP and BLTP, 141980 Dubna, Russia

E-mail: Michael.Ilgenfritz@sunse.jinr.ru

M. Kalinowski

*Goethe-Universität Frankfurt am Main, Institut für Theoretische Physik, 60438 Frankfurt
am Main, Germany*

E-mail: kalinowm@th.physik.uni-frankfurt.de

In this talk we report on our study of two-colour lattice QCD with $N_f = 4$ staggered fermion degrees of freedom with equal electric charge q in a homogeneous magnetic field B at non-zero temperature T . We find indications for a non-monotonic behaviour of the critical temperature as a function of the magnetic field strength and, as a consequence, for the occurrence of *inverse magnetic catalysis* within the transition region for magnetic fields in the range $0 \leq qB \lesssim 0.7 \text{ GeV}^2$.

*QCD-TNT-III-From quarks and gluons to hadronic matter: A bridge too far?,
2-6 September, 2013*

European Centre for Theoretical Studies in Nuclear Physics and Related Areas (ECT),
Villazzano, Trento (Italy)*

^{*}Speaker.

[†]MMP expresses his gratitude to the organizers for having been invited to this interesting workshop and to the ECT* staff for kind hospitality.

1. Introduction

The behaviour of hadronic matter under the influence of a strong magnetic field B has recently been widely discussed because of its relevance for non-central heavy ion collisions. In such collisions there will be two lumps of spectators moving in opposite directions. They give rise to a magnetic field perpendicular to the reaction plane. It can be shown that the magnetic field is so strong that its consequences cannot be studied perturbatively [1, 2, 3].

The influence of an external magnetic field on hadronic matter at zero temperature has been studied by various authors, e.g. within the Nambu-Jona-Lasinio [4] or in the chiral model [5]. The general result is that the magnetic field induces an increase of the chiral condensate. This was called *magnetic catalysis* in [6] and claimed to be essentially model independent. For a recent review see also [7]. The model calculations have been extended also to finite temperature T , in order to study the phase diagram of strongly interacting matter in a constant magnetic field. The critical temperature of the chiral phase transition rises in most of the calculations [8, 9]. But there are also claims that the chiral and the deconfinement phase transitions may split, and the critical temperature of the latter decreases with the magnetic field strength [10, 11, 12, 13].

A couple of years ago several groups have started to investigate the problem through *ab initio* lattice simulations of QCD and QCD-like theories with a homogenous magnetic background field. The pioneering work - employing quenched $SU(2)$ - was performed by M. Polikarpov † and his collaborators [14, 15]. Later on, a few groups have performed investigations in full lattice QCD (in Pisa [16, 17], in Regensburg [18, 19, 20, 21], see also [22] and very recently [23]). All groups observe magnetic catalysis for temperatures in the confined phase. In the transition or (better) crossover region the Regensburg group reported what they call *inverse magnetic catalysis*, i.e. the chiral condensate and thus the (pseudo-)critical temperature decrease with increasing magnetic field strength. A nice recent review of the lattice results for QCD and QCD-like theories in external fields can be found in Ref. [24].

In this talk we report on our two-colour QCD investigations [25, 26] with $N_f = 4$ flavour fermion degrees of freedom with equal electric charges (avoiding any “rooting” of the fermionic determinant). In this case a first order finite temperature transition [27] can be expected in contrast to the observed smooth crossover for $N_f = 2$ or $2 + 1$ at small but non-vanishing u -, d -quark masses. Although our model is not QCD, the chiral properties are quite similar. Furthermore, investigations of the dynamical $SU(2)$ theory are of considerable interest, because they can be extended to finite chemical potential without a sign problem.

In Section 2 we specify the action and our observables as well as the setup for our simulations. In Section 3 we discuss the temperature and magnetic field dependence of the Polyakov loop and chiral condensate as well as of their respective susceptibilities. Moreover, we provide results of a recent fixed-scale study at smaller quark mass. In Section 4 we provide a conjecture about the $B - T$ phase diagram and on the occurrence of (inverse) magnetic catalysis.

2. Setup of the lattice investigation

We introduce a lattice of four-dimensional size $\mathcal{V} \equiv N_\tau \times N_\sigma^3$ with a spacing unit a . The physical volume and temperature are $V = (aN_\sigma)^3$ and $T = 1/(aN_\tau)$, respectively. On the links $n \rightarrow n + \hat{\mu}$ the group elements $U_\mu(n) \in SU(2)$, $\mu = 1, 2, 3, 4$ are defined. Periodic boundary conditions are assumed. We employ the standard Wilson plaquette action

$$S_G = \beta \mathcal{V} \sum_{\mu < \nu} P_{\mu\nu}, \quad P_{\mu\nu} = \frac{1}{\mathcal{V}} \sum_n \left(\frac{1}{2} \text{Tr}(\mathbf{1} - U_{\mu\nu}(n)) \right) \quad (2.1)$$

with $U_{\mu\nu}(n)$ denoting the $\mu\nu$ -plaquette matrix at site n . For the fermion part of the action, we use staggered Grassmann variables $\bar{\chi}_n$ and χ_n transforming with the fundamental representation of the gauge group $SU(2)$. For simplicity the four flavour degrees of freedom are assumed to carry equal electric charges q allowing to interact with an external magnetic field B . The boundary conditions of the fermionic fields are (anti-) periodic in the space (time) directions. In the absence of a magnetic field the fermionic part of the action reads

$$S_F = a^3 \sum_{n, n'} \bar{\chi}_n [D_{n, n'} + ma\delta_{n, n'}] \chi_{n'}, \quad D_{n, n'} = \frac{1}{2} \sum_\mu \eta_\mu(n) [U_\mu(n) \delta_{n+\mu, n'} - U_\mu^\dagger(n-\mu) \delta_{n-\mu, n'}], \quad (2.2)$$

where m is the bare quark mass. The $\eta_\mu(n)$ are the standard staggered sign factors,

$$\eta_1(n) = 1, \quad \eta_\mu(n) = (-1)^{\sum_{\nu=1}^{\mu-1} n_\nu}, \quad \mu = 2, 3, 4. \quad (2.3)$$

We introduce electromagnetic background potentials into the fermion action by new, commuting group elements on the links, namely $V_\mu(n) = e^{i\theta_\mu(n)} \in U(1)$. A constant magnetic background field in the $z \equiv 3$ -direction penetrating through all the $(x, y) \equiv (1, 2)$ -planes of finite size $N_\sigma \times N_\sigma$ with a constant magnetic flux $\phi = a^2 q B$ through each plaquette can be realized as follows:

$$\begin{aligned} V_1(n) &= e^{-i\phi n_2/2} \quad (n_1 = 1, 2, \dots, N_\sigma - 1), & V_2(n) &= e^{i\phi n_1/2} \quad (n_2 = 1, 2, \dots, N_\sigma - 1), \\ V_1(N_\sigma, n_2, n_3, n_4) &= e^{-i\phi(N_\sigma+1)n_2/2}, & V_2(n_1, N_\sigma, n_3, n_4) &= e^{i\phi(N_\sigma+1)n_1/2}, \\ V_3(n) &= V_4(n) = 1. \end{aligned} \quad (2.4)$$

With periodic boundary conditions the magnetic flux becomes quantized as $\phi = a^2 q B = 2\pi N_b / N_\sigma^2$, $N_b \in \mathbb{Z}$. Because the angle ϕ is periodic, the flux is bounded from above $\phi < \pi$. One obtains the condition $N_b < N_\sigma^2/2$. Physically reasonable strong fields should then be restricted at least to half of this bound, i.e. $N_b \leq N_\sigma^2/4$.

We introduce the fields $V_\mu(\theta)$ into the fermionic action $S_F(\theta)$ by substituting in Eq. (2.2)

$$U_\mu(n) \rightarrow V_\mu(n) U_\mu(n), \quad U_\mu^\dagger(n) \rightarrow V_\mu^*(n) U_\mu^\dagger(n). \quad (2.5)$$

The partition function in the background field θ is then given by

$$Z(\theta) = \int \prod (d\bar{\chi}(n) d\chi(n) dU_\mu(n)) e^{-S_G - S_F(\theta)}. \quad (2.6)$$

The simulation algorithm employed is the usual Hybrid Monte Carlo method, updated in various respects in order to increase efficiency (even-odd and mass preconditioning, multiple time scales, Omelyan integrator and written in CUDA Fortran for the use on GPU's).

We have computed the average Polyakov loop $\langle L \rangle$, which is the order parameter for confinement in the limit of infinite quark mass

$$\langle L \rangle = \frac{1}{N_\sigma^3} \sum_{n_1, n_2, n_3} \frac{1}{2} \langle \text{Tr} \left(\prod_{n_4=1}^{N_\tau} U_4(n_1, n_2, n_3, n_4) \right) \rangle \quad (2.7)$$

and its susceptibility $\chi_L = N_\sigma^3 (\langle L^2 \rangle - \langle L \rangle^2)$. The chiral condensate, which is an exact order parameter in the limit of vanishing quark mass, is given by

$$a^3 \langle \bar{\chi} \chi \rangle = -\frac{1}{\gamma} \frac{1}{4} \frac{\partial}{\partial (ma)} \log(Z) = \frac{1}{\gamma} \frac{1}{4} \langle \text{Tr}(D + ma)^{-1} \rangle. \quad (2.8)$$

In order to locate the phase transition we have used also the disconnected part of the susceptibility (called ‘‘chiral susceptibility’’ for simplicity),

$$\chi = \frac{1}{N_\tau N_\sigma^3} \frac{1}{4} \frac{\partial^2}{(\partial (ma))^2} \log(Z) = \chi_{\text{conn}} + \chi_{\text{disc}}, \quad (2.9)$$

$$\chi_{\text{disc}} = \frac{1}{N_\tau N_\sigma^3} \frac{1}{16} (\langle (\text{Tr}(D + ma)^{-1})^2 \rangle - \langle \text{Tr}(D + ma)^{-1} \rangle^2). \quad (2.10)$$

It is important to notice that the mean values defined above are bare quantities which in principle should be renormalized when comparing with continuum expectation values.

To study the influence of an external magnetic field we have also computed the anisotropy in the gluonic action by measuring the average value $\langle P_{\mu\nu} \rangle$ of the non-Abelian plaquette energies for the different $\mu - \nu$ planes as a function of the magnetic field strength and of the temperature.

A zero-temperature simulation without magnetic field was performed for $\beta = 1.80$ and for the two mass values $ma = 0.0025, 0.01$ on a lattice of size $32^3 \times 48$ in order to estimate the lattice spacing and the pion mass (for details see [25, 26]).

For the determination of the lattice spacing a we have computed the potential between infinitely heavy quarks. From this we obtained the Sommer parameter, defined in the continuum by the equation

$$r^2 \frac{dV}{dr} \Big|_{r=r_0} = 1.65. \quad (2.11)$$

Assuming $r_0 = 0.468(4)$ fm [28] the lattice spacings for $ma = 0.0025$ and $ma = 0.01$ were obtained (cf. Table 1). Inserting the value of a into the result for the effective pseudo-scalar meson mass we obtained the pion mass in physical units for $ma = 0.0025$ and about half of that value for $ma = 0.01$ as expected from the relation $m_\pi^2 \propto m$ (cf. Table 1). As a consequence, for $am = 0.01$ we reached a ratio $m_\pi/T_c(B=0) \approx 1.7$, which is similar to the estimate in [16, 17], but higher than that in [18]. However, for $am = 0.0025$ we gained a value $m_\pi/T_c(B=0) \approx 1.0$ already interesting for a comparison with the real physical situation.

β	am	N_σ	N_τ	N_b^m	R_0	a [fm]	m_π [MeV]	$\sqrt{q\bar{B}_m}$ [GeV]
1.8	.01	16	32	50	2.75(8)	0.170(5)	330(10)	1.29(4)
1.8	.0025	32	48	200	2.78(6)	0.168(4)	175(4)	1.30(3)

Table 1: Results for the Sommer scale R_0 (in lattice units), the lattice spacing a , the pion mass m_π , and the magnetic field strength $\sqrt{q\bar{B}_m}$ for N_b^m flux units [25, 26].

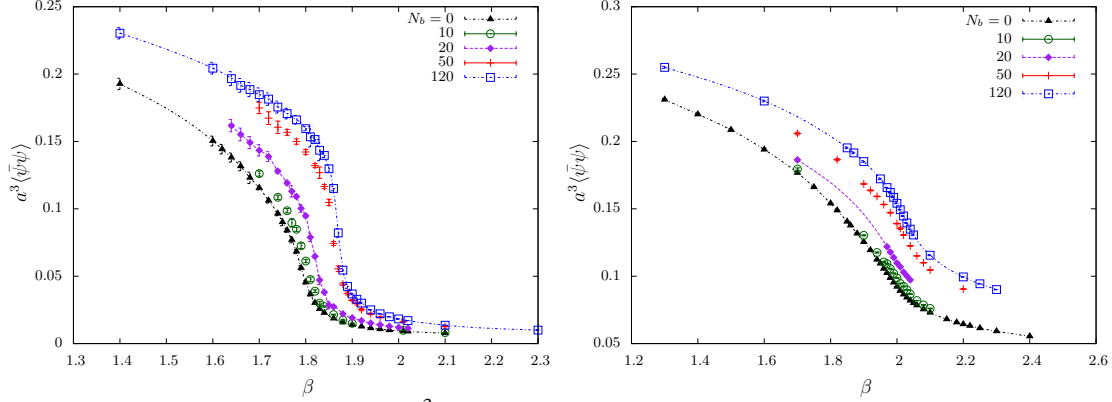


Figure 1: Bare chiral condensate $a^3\langle\bar{\psi}\psi\rangle$ vs. β for various magnetic fluxes ϕ (in flux units), $ma = 0.01$ (left panel) and $ma = 0.1$ (right panel), lattice size $16^3 \times 6$. Curves are to guide the eye.

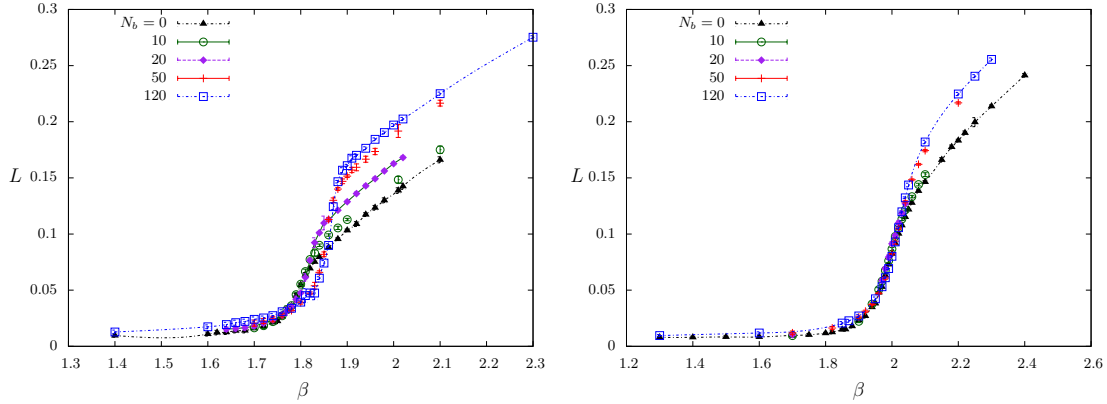


Figure 2: Same as for Fig. 1 but for the bare Polyakov loop $\langle L \rangle$ vs. β .

3. Results

In Fig. 1 we have plotted the bare chiral condensate as a function of β for a set of numbers of flux quanta and for the bare quark mass values $ma = 0.01$ (left panel) and $ma = 0.1$ (right panel). In both of the cases the chiral condensate increases with rising magnetic field for arbitrary fixed β . For the smaller quark mass we see quite clearly a transition for all values of the flux quanta N_b under consideration. Moreover, the chiral transition seems to move to higher temperatures as the magnetic field is increasing. This tendency is in agreement with the results in [16, 17] but opposite to [18], where the chiral condensate was seen to decrease with the flux ϕ in the transition region, leading to a decrease of the transition temperature. In Fig. 2 the expectation value of the Polyakov loop is shown vs. β for the same two values of the bare quark mass. The transition temperature obviously increases with the quark mass as expected. At the high quark mass there

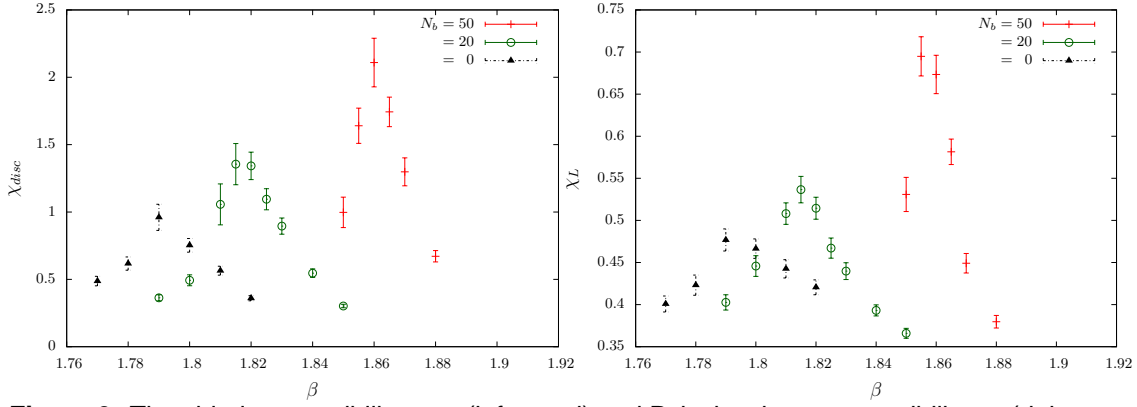


Figure 3: The chiral susceptibility χ_{disc} (left panel) and Polyakov loop susceptibility χ_L (right panel) vs. β at $am = 0.01$ for magnetic fluxes N_b at lattice size $16^3 \times 6$.

seems to be only a weak effect of the magnetic field on the deconfinement temperature. At the smaller mass value we observe a non-monotonic behaviour with the magnetic field for fixed β -values within the transition region. In Fig. 3 we show the chiral susceptibility and the Polyakov loop susceptibility for the lower quark mass value $ma = 0.01$. It is clearly seen in the left figure that the chiral transition indeed moves to higher temperatures as the magnetic field becomes stronger. In the right figure we show the same effect for the Polyakov loop susceptibility. The maxima of the two susceptibilities turn out to be at the same value for given magnetic field. Thus, there is no sign of a splitting between the chiral and the deconfinement transition as it should be expected for a real phase transition. However, let us keep in mind that the rise of the temperature $T = 1/a(\beta)N_\tau$ by lowering $a(\beta)$ causes the physical values of the mass m and of the magnetic field qB to increase as well, since their values remained fixed only in lattice units. At the same time we did not renormalize our observables. Below we demonstrate how to circumvent these obstacles.

In order to study the dependence of the chiral condensate on the magnetic field strength in the chiral limit, we have looked at the behaviour of the chiral condensate as a function of the quark mass and of the magnetic field for various β 's. Because we now keep β fixed we eliminate lattice effects coming from the variation of a . We have considered $\beta = 1.70$ (confined phase), $\beta = 1.90$ (transition region), and $\beta = 2.10$ (deconfined phase). In the left panel of Fig. 4 we show the dependence of the bare chiral condensate on the quark mass for various values of magnetic flux at $\beta = 1.70$. To obtain the results relevant to continuum physics, one has to subtract an additive divergence for finite quark mass, as well as do a multiplicative renormalization, which is needed also at zero mass. In the right panel of Fig. 4 we show the difference between the bare chiral condensate for finite fluxes subtracted by the same quantity at zero flux. This eliminates the main part of the additive divergence. In the left panel we have also included points at vanishing quark mass, where there are no additive divergencies. The non-vanishing values in this limit are obtained by a chiral extrapolation. Because we are not very far from the transition, we have supposed a behaviour as for the reduced three-dimensional model [27]

$$a^3 \langle \bar{\psi}\psi \rangle = a_0 + a_1 \sqrt{ma} + a_2 ma. \quad (3.1)$$

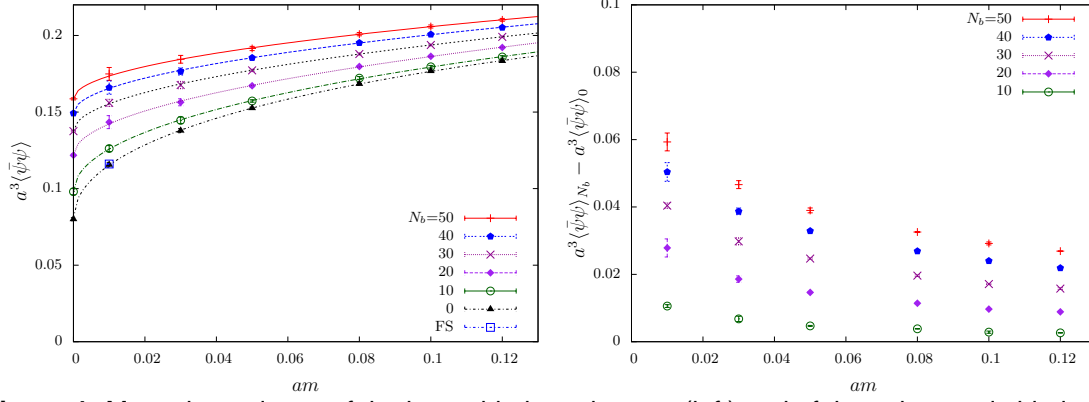


Figure 4: Mass dependence of the bare chiral condensate (left) and of the subtracted chiral condensate (right) for various magnetic fluxes at $\beta = 1.70$ (confinement). Lattice size is $16^3 \times 6$ (FS denotes a finite-size check for $qB = 0$ with $24^3 \times 6$). Lines show fits with Eq. (3.1).

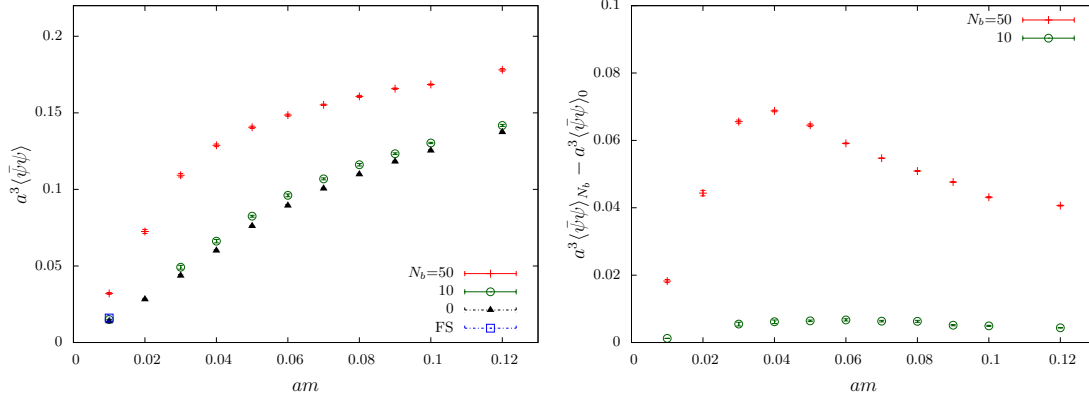


Figure 5: Same as for Fig. 4 but in the transition region ($\beta = 1.90$).

Thus, we clearly see chiral symmetry breaking for $\beta = 1.70$. In Fig. 5 we show the mass dependence of the bare chiral condensate (left panel) and the subtracted chiral condensate (right panel) in the transition region (at $\beta = 1.90$) for three values of the magnetic flux. One can see that for finite flux, as well as for zero flux, the bare and subtracted chiral condensates are consistent with extrapolating to zero in the chiral limit. For the highest flux, $N_b = 50$ one can clearly discern two regions of behaviour. For $am \gtrsim 0.04$ the chiral condensate seems to extrapolate to a finite value, but for $am \lesssim 0.04$ it actually extrapolates to zero. This can be understood, if one assumes that the transition for $N_b = 50$ at this value of β takes place for $am \approx 0.04$. In Fig. 6 we present the same quantities as above, but for $\beta = 2.10$. This is well inside the chirally restored phase. The chiral condensate extrapolates to zero for all values of the flux. Thus, chiral symmetry is restored for all values of the flux that we have investigated.

In our recent investigation [26] we have used a fixed-scale approach, i.e. we kept β fixed and thereby the lattice spacing a and varied the temperature by changing N_τ . In this way we may easily fix the mass value as well as the magnetic field strength, while varying the temperature. Moreover, for the time being we may neglect renormalization effects. More precisely we simulated the theory at $\beta = 1.80$ mainly with lattice sizes $32^3 \times N_\tau$, $N_\tau =$

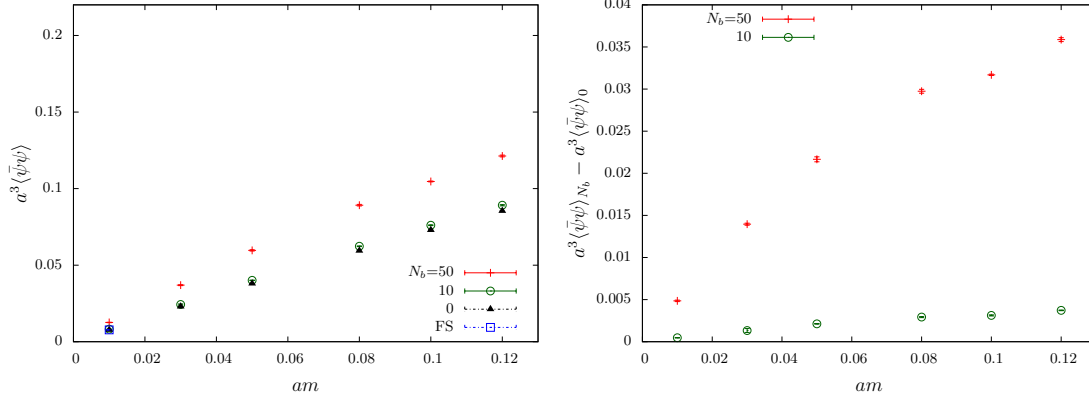


Figure 6: Same as for Fig. 4 but in the deconfinement phase ($\beta = 2.1$).

4, 6, 8, 10, and with an even lower mass value $ma = 0.0025$ (cf. Table 1) taking each time as a minimum three values of the magnetic flux $qB = 0.0, 0.67, 1.69 \text{ GeV}^2$ corresponding to flux unit numbers $N_b = 0, 80, 200$, respectively.

The influence of the magnetic field on the gauge field can be represented by studying the different parts $P_{\mu\nu}$ of the gluonic action. We introduce variables as in [20]

$$\mathcal{E}_i^2 = \langle P_{4i} \rangle, \quad \mathcal{B}_i^2 = |\varepsilon_{ijk}| \langle P_{jk} \rangle, \quad j < k. \quad (3.2)$$

At $B = T = 0$ they are all equal by symmetry. At $B = 0, T \neq 0$ they fall into two groups, because the fourth direction is not equivalent to the other ones:

$$\mathcal{E}_1^2 = \mathcal{E}_2^2 = \mathcal{E}_3^2 \leq \mathcal{B}_1^2 = \mathcal{B}_2^2 = \mathcal{B}_3^2. \quad (3.3)$$

Introducing a magnetic field in the third direction, for $T \neq 0$ the only symmetries left are rotations in the (1,2)-plane. We therefore may define

$$\mathcal{E}_{\parallel}^2 \equiv \mathcal{E}_3^2, \quad \mathcal{E}_{\perp}^2 \equiv \mathcal{E}_1^2 = \mathcal{E}_2^2, \quad \mathcal{B}_{\parallel}^2 \equiv \mathcal{B}_3^2, \quad \mathcal{B}_{\perp}^2 \equiv \mathcal{B}_1^2 = \mathcal{B}_2^2. \quad (3.4)$$

In Fig. 7 we show the results for the four temperature values, and each of them for the three values of the magnetic field. We can see the following features from this figure. The

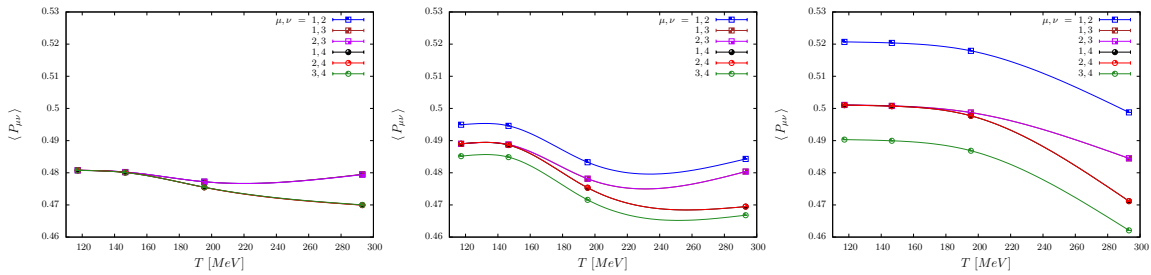


Figure 7: Plaquette energies $\langle P_{\mu\nu} \rangle$ vs. temperature $T = (a(\beta)N_{\tau})^{-1}$ for $qB = 0$ (left), $qB = 0.67 \text{ GeV}^2$ (middle), and $qB = 1.69 \text{ GeV}^2$ (right) for different plaquette orientations ($\beta = 1.80, am = 0.0025, N_{\sigma} = 32$). Lines are to guide the eye.

pattern of the splitting is the same as in our previous article [25] and more recently found

in full QCD [20],

$$\mathcal{B}_{\parallel}^2 \geq \mathcal{B}_{\perp}^2 \geq \mathcal{E}_{\perp}^2 \geq \mathcal{E}_{\parallel}^2. \quad (3.5)$$

Furthermore, if $\mathcal{B}_{\perp}^2 - \mathcal{E}_{\perp}^2 > 0$ – which can be interpreted as a contribution to the entropy – the system can be expected to be at the onset of the deconfinement transition or even inside the deconfined phase. If we compare the middle panel ($qB = 0.67 \text{ GeV}^2$) of Fig. 7 with the left one ($qB = 0$) then at $T = 195 \text{ MeV}$ ($N_{\tau} = 6$) we find this difference to be slightly larger than for the left panel. This might be an indication that the transition temperature as a function of the temperature went down a bit with increasing magnetic field strength. However, comparing the right panel ($qB = 1.69 \text{ GeV}^2$) with the left one, then the corresponding difference is definitely smaller than for zero magnetic field. This indicates that the transition might be shifted to a higher temperature value.

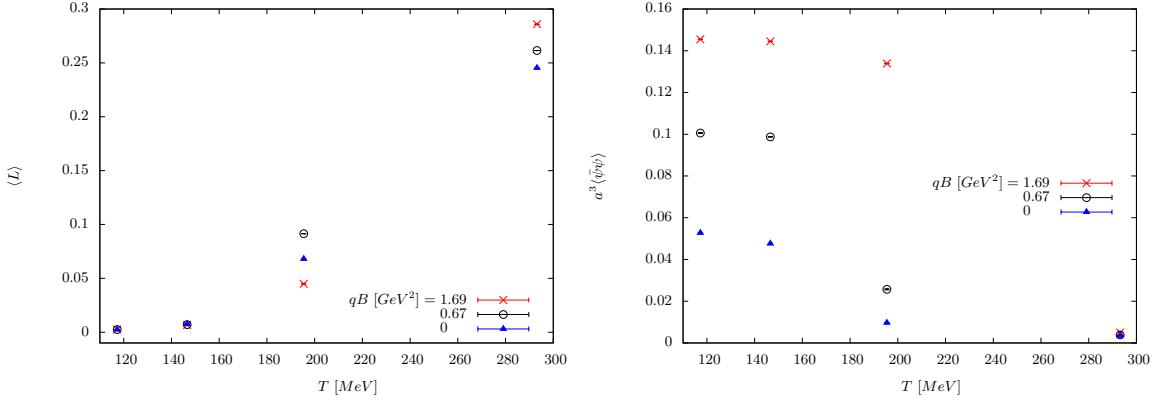


Figure 8: Bare Polyakov loop $\langle L \rangle$ (left) and bare chiral condensate $\langle \bar{\psi} \psi \rangle$ (right) vs. $T = (a(\beta)N_{\tau})^{-1}$ for three values of the magnetic field strength at $\beta = 1.80$, $am = 0.0025$ and $32^3 \times N_{\tau}$, $N_{\tau} = 4, 6, 8, 10$.

In Fig. 8 (left) the expectation value of the unrenormalized Polyakov loop $\langle L \rangle$ is shown as a function of the temperature. Our sizes $N_{\tau} = 4, \dots, 10$ correspond to temperature values T , which are quite widely spaced. Therefore, we cannot localize the transition e.g. for $B = 0$ very well. It happens around $T = T_c \simeq 160 - 190 \text{ MeV}$. At $T = 195 \text{ MeV}$ ($N_{\tau} = 6$) we clearly observe again, that the Polyakov loop does not behave monotonously with the magnetic field (see also [16]). In Fig. 8 (right) the unrenormalized chiral order parameter $a^3 \langle \bar{\psi} \psi \rangle$ is shown versus T . For a fixed non-vanishing quark mass it is increasing monotonously with the magnetic field at least for the three lower temperature values we have investigated. This might mean that T_c always increases with a rising magnetic field strength as required for the *magnetic catalysis*. In particular at $T = 195 \text{ MeV}$ we observe a strong increase of the condensate between $qB = 0.67 \text{ GeV}^2$ and our largest value 1.69 GeV^2 indicating that the system ‘jumps’ from chiral symmetry restoration to the chirally broken phase. This indicates that at this temperature value and within the given range of magnetic field strength values the critical $T_c(B)$ is rising. We find this confirmed, as previously shown in Fig. 5 corresponding to the transition region. At the temperature $T = 195 \text{ MeV}$ ($N_{\tau} = 6$) the chiral extrapolation of the condensate $a^3 \langle \bar{\psi} \psi \rangle$ for $qB = 0$ and $qB = 0.67 \text{ GeV}^2$ points to zero, i.e. to the chirally restored phase, while for the stronger magnetic field strength 1.69 GeV^2 the data suggest a non-vanishing chiral condensate in the chiral limit (see [26]). Thus, we

may conclude that at very strong magnetic field values the transition temperature grows with B . This means *magnetic catalysis* in agreement with various models [7].

In order to study the situation in more detail, we have made simulations at the same temperature $T = 195$ MeV with a few more values of N_b . The latter correspond to a range of qB between 0 and 1.69 GeV^2 . We measure the expectation values of the Polyakov loop and the chiral condensate. The results are shown in Fig. 9. There is a sharp change, which

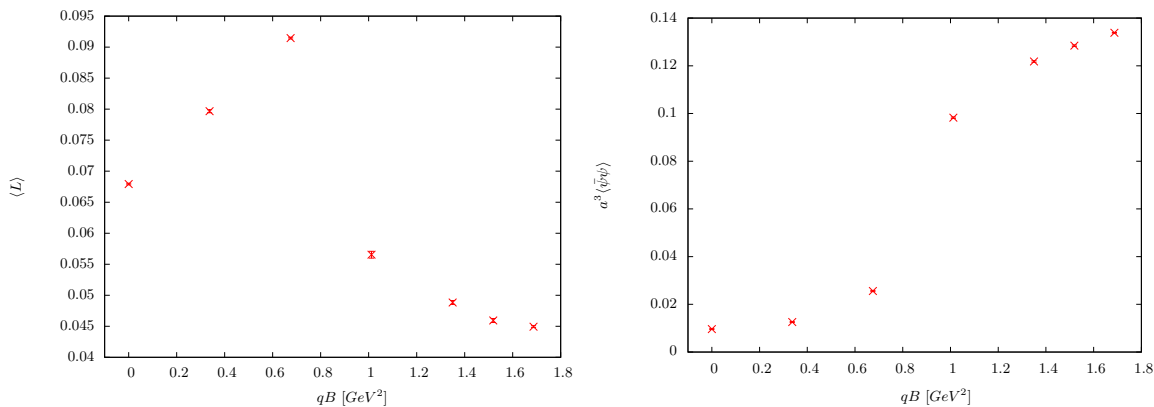


Figure 9: Polyakov loop (left panel) and chiral condensate (right panel) vs. field strength qB at $T = 195$ MeV obtained with $\beta = 1.80$, $am = 0.0025$ and $32^3 \times 6$.

might be related to a phase transition in the range $0.7 \text{ GeV}^2 < qB < 1.0 \text{ GeV}^2$ corresponding to $\sqrt{qB}/T \approx 4.5$. This observation is supporting a *magnetic catalysis* phenomenon. But for lower magnetic fields we observe a rise of the Polyakov loop with qB towards the transition and only then a drop off followed by a monotonous decrease at larger field values (compare with our previous non-monotonicity comment to Fig. 8 (left)). The rise at low magnetic field values might mean that we are going deeper into the deconfinement region, after which the transition brings us back into the confinement or chirally broken phase. The observation of the rise of the Polyakov loop at low magnetic field values resembles the pattern discussed in Refs. [21], where it was related to the *inverse magnetic catalysis* phenomenon.

4. Conclusions

Our observations above seem to indicate a decrease of T_c with rising but small qB . At large qB the transition temperature T_c definitely rises as expected in the case of a magnetic catalysis. In Fig. 10 we conjecture a $B - T$ phase diagram, which might clarify the situation. In order to prove it, further simulations at somewhat smaller temperatures and/or smaller quark mass would be helpful. If it proves to be true then one finds temperature values, where at $qB = 0$ the system is in the confinement (chirally broken) phase. With increasing qB one passes then the chirally restored phase, i.e. the deconfinement or chiral transition twice, and ends up again in the confinement phase. Along such a path in the phase diagram the chiral condensate should decrease with qB when entering the

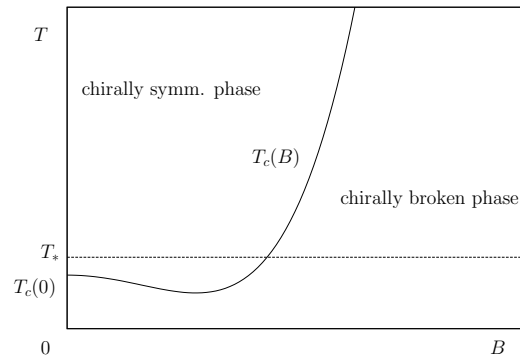


Figure 10: Conjectured B-T phase diagram at fixed mass $am = 0.0025$. The horizontal line $T = T_* = \text{const.}$ indicates the path of simulations at $T = 195$ MeV as in Fig 9.

chirally restored phase. This would mean the existence of *inverse magnetic catalysis* also in two-colour QCD considered throughout this work [25, 26].

References

- [1] D. Kharzeev, L. McLerran, and H. Warringa, “The Effects of topological charge change in heavy ion collisions: ‘Event by event P and CP violation’,” *Nucl.Phys.* **A803** (2008) 227, arXiv:0711.0950 [hep-ph].
- [2] V. Skokov, A. Illarionov, and V. Toneev, “Estimate of the magnetic field strength in heavy-ion collisions,” *Int.J.Mod.Phys.* **A24** (2009) 5925, arXiv:0907.1396 [nucl-th].
- [3] L. McLerran and V. Skokov, “Comments about the electromagnetic field in heavy-ion collisions,” arXiv:1305.0774 [hep-ph].
- [4] S. Klevansky and R. Lemmer, “Chiral symmetry restoration in the Nambu-Jona-Lasinio model with a constant electromagnetic field,” *Phys.Rev.* **D39** (1989) 3478.
- [5] I. Shushpanov and A. Smilga, “Quark condensate in a magnetic field,” *Phys.Lett.* **B402** (1997) 351, arXiv:hep-ph/9703201 [hep-ph].
- [6] V. Gusynin, V. Miransky, and I. Shovkovy, “Catalysis of dynamical flavor symmetry breaking by a magnetic field in (2+1)-dimensions,” *Phys.Rev.Lett.* **73** (1994) 3499–3502, arXiv:hep-ph/9405262 [hep-ph].
- [7] I. A. Shovkovy, “Magnetic catalysis: A review,” *Lect.Notes Phys.* **871** (2013) 13–49, arXiv:1207.5081 [hep-ph].
- [8] K. Klimenko, “Three-dimensional Gross-Neveu model at nonzero temperature and in an external magnetic field,” *Theor.Math.Phys.* **90** (1992) 1.
- [9] N. Agasian, “Chiral thermodynamics in a magnetic field,” *Phys.Atom.Nucl.* **64** (2001) 554, arXiv:hep-ph/0112341 [hep-ph].
- [10] N. Agasian and S. Fedorov, “Quark-hadron phase transition in a magnetic field,” *Phys.Lett.* **B663** (2008) 445, arXiv:0803.3156 [hep-ph].
- [11] A. Mizher, M. Chernodub, and E. Fraga, “Phase diagram of hot QCD in an external magnetic field: possible splitting of deconfinement and chiral transitions,” *Phys.Rev.* **D82** (2010) 105016, arXiv:1004.2712 [hep-ph].

- [12] A. Amador and J. O. Andersen, “Two-color QCD in a strong magnetic field: The role of the Polyakov loop,” *Phys.Rev.* **D88** (2013) 025016, arXiv:1211.7293 [hep-ph].
- [13] V. Orlovsky and Y. A. Simonov, “Quark mass dependence of the QCD temperature transition in magnetic fields,” arXiv:1312.4178 [hep-ph].
- [14] P. Buividovich, M. Chernodub, E. Luschevskaya, and M. Polikarpov, “Numerical study of chiral symmetry breaking in non-Abelian gauge theory with background magnetic field,” *Phys.Lett.* **B682** (2010) 484, arXiv:0812.1740 [hep-lat].
- [15] P. Buividovich, M. Chernodub, E. Luschevskaya, and M. Polikarpov, “Chiral magnetization of non-Abelian vacuum: A Lattice study,” *Nucl.Phys.* **B826** (2010) 313, arXiv:0906.0488 [hep-lat].
- [16] M. D’Elia, S. Mukherjee, and F. Sanfilippo, “QCD phase transition in a strong magnetic background,” *Phys.Rev.* **D82** (2010) 051501, arXiv:1005.5365 [hep-lat].
- [17] M. D’Elia and F. Negro, “Chiral properties of strong interactions in a magnetic background,” *Phys.Rev.* **D83** (2011) 114028, arXiv:1103.2080 [hep-lat].
- [18] G. Bali, F. Bruckmann, G. Endrodi, Z. Fodor, S. Katz, *et al.*, “The QCD phase diagram for external magnetic fields,” *JHEP* **1202** (2012) 044, arXiv:1111.4956 [hep-lat].
- [19] G. Bali, F. Bruckmann, G. Endrodi, Z. Fodor, S. Katz, and A. Schäfer, “QCD quark condensate in external magnetic fields,” *Phys.Rev.* **D86** (2012) 071502, arXiv:1206.4205 [hep-lat].
- [20] G. Bali, F. Bruckmann, G. Endrodi, F. Gruber, and A. Schäfer, “Magnetic field-induced gluonic (inverse) catalysis and pressure (an)isotropy in QCD,” *JHEP* **1304** (2013) 130, arXiv:1303.1328 [hep-lat].
- [21] F. Bruckmann, G. Endrodi, and T. Kovacs, “Inverse magnetic catalysis and the Polyakov loop,” *JHEP* **1304** (2013) 112, arXiv:1303.3972 [hep-lat].
- [22] L. Levkova and C. DeTar, “Quark-gluon plasma in an external magnetic field,” arXiv:1309.1142 [hep-lat].
- [23] V. Bornyakov, P. Buividovich, N. Cundy, O. Kochetkov, and A. Schäfer, “Deconfinement transition in two-flavour lattice QCD with dynamical overlap fermions in an external magnetic field,” arXiv:1312.5628 [hep-lat].
- [24] M. D’Elia, “Lattice QCD simulations in external background fields,” *Lect.Notes Phys.* **871** (2013) 181–208, arXiv:1209.0374 [hep-lat].
- [25] E.-M. Ilgenfritz, M. Kalinowski, M. Müller-Preussker, B. Petersson, and A. Schreiber, “Two-color QCD with staggered fermions at finite temperature under the influence of a magnetic field,” *Phys.Rev.* **D85** (2012) 114504, arXiv:1203.3360 [hep-lat].
- [26] E.-M. Ilgenfritz, M. Müller-Preussker, B. Petersson, and A. Schreiber, “Magnetic catalysis (and inverse catalysis) at finite temperature in two-color lattice QCD,” arXiv:1310.7876 [hep-lat].
- [27] R. D. Pisarski and F. Wilczek, “Remarks on the chiral phase transition in chromodynamics,” *Phys.Rev.* **D29** (1984) 338.
- [28] A. Bazavov, T. Bhattacharya, M. Cheng, C. DeTar, H. Ding, *et al.*, “The chiral and deconfinement aspects of the QCD transition,” *Phys.Rev.* **D85** (2012) 054503, arXiv:1111.1710 [hep-lat].